Dendrimer Generation Effects on Photodynamic Efficacy of Dendrimer Porphyrins and Dendrimer-Loaded Supramolecular Nanocarriers

Yuan Li,[†] Woo-Dong Jang,*[,‡] Nobuhiro Nishiyama,[§] Akihiro Kishimura,[†,+,@] Satoko Kawauchi,[||] Yuji Morimoto,[||] Sayaka Miake,[⊥] Takashi Yamashita,[⊥] Makoto Kikuchi,[||] Takuzo Aida,[#,@] and Kazunori Kataoka*[,†,§,+,@]

Department of Materials Engineering, Graduate School of Engineering, The University of Tokyo, 7-3-1 Hongo, Bunkyo-ku, Tokyo 113-8656, Japan, Department of Chemistry, College of Science, Yonsei University, 134 Sinchondong, Seodaemun-gu, Seoul 120-749, Korea, Center for Disease Biology and Integrative Medicine, Graduate School of Medicine, The University of Tokyo, 7-3-1 Hongo, Bunkyo-ku, Tokyo 113-0033, Japan, Department of Medical Engineering, National Defense Medical College, 3-2 Namiki, Tokorozawa, Saitama 359-8513, Japan, Department of Pure and Applied Chemistry, Faculty of Science and Technology, Tokyo University of Science, 2641 Yamazaki, Noda-shi, Chiba 278-8510, Japan, Department of Chemistry and Biotechnology, Graduate School of Engineering, The University of Tokyo, 7-3-1 Hongo, Bunkyo-ku, Tokyo 113-8656, Japan, Core Research for Evolutional Science and Technology (CREST), Japan Science and Technology Agency (JST), and Center for NanoBio Integration, The University of Tokyo, 7-3-1 Hongo, Bunkyo-ku, Tokyo 113-8656, Japan

Received May 29, 2007. Revised Manuscript Received July 17, 2007

A series of poly(benzyl ether) dendrimer porphyrins (DPs) (Gn = n-generation dendrimer, n = 1−3) was examined as potential photosensitizers for photodynamic therapy (PDT). Polyion complexes (PICs) between the DPs and poly(ethylene glycol)-*block*-poly(L-lysine) (PEG-*b*-PLL) were formed via an electrostatic interaction between the positively charged poly(L-lysine) (PLL) segment and negatively charged periphery of the DPs. Dynamic light scattering (DLS) measurements and transmission electron microscopy (TEM) showed that G3 formed a core−shell-type nanocarrier micelle, whereas G1 and G2 formed irregular-shaped nanoparticles with a relatively high polydispersity. The photophysical properties of the DP-loaded PIC nanocarriers strongly depend on the generation of the DPs. In the case of G1 and G2, their fluorescence lifetime and oxygen consumption ability were significantly reduced by the formation of the PIC nanocarriers, whereas the G3-loaded PIC nanocarrier exhibited almost comparable fluorescence lifetimes and oxygen consumption abilities to the free G3. The incorporation of DPs into PIC nanocarriers resulted in an appreciable increase in the cellular uptake, yet inversely correlated with the generation. Alternatively, the photocytotoxicity of the DPs within the nanocarriers increased with an increase in the generation despite a decrease in the cellular uptake. By correlating the effects of the uptake amount with the photocytotoxicity, the PIC nanocarriers showed remarkable enhancement of the PDT efficacy dependent on the generation of DPs.

Introduction

Dendrimers with predictable three-dimensional architectures are currently undergoing fast growth in various applications. This is due in part to the variety of applications being pursued for dendrimers.[1,2] In particular, application of dendrimers to biomedical uses has attracted much attention due to the tunable properties of the dendrimer generation, terminal groups, and inner cavity for the incorporation of a variety of molecules.[1−6] PAMAM dendrimers, for example, have been comprehensively investigated as diagnostic tools and drug carriers.[6−8] Recently, we have reported the third generation poly(benzyl ether) dendrimer porphyrins (DPs) as an effective photosensitizer for photodynamic therapy (PDT).[9−11]

PDT involves the administration of a photosensitizer, which preferentially accumulates in target tissues. Subsequent

* To whom correspondence should be addressed. Phone: +81-3-5841-7138. Fax: +81-3-5841-7139. E-mail: kataoka@bmw.t.u-tokyo.ac.jp.
[†] Department of Materials Engineering, The University of Tokyo.
[‡] Yonsei University.
[§] Center for Disease Biology and Integrative Medicine, The University of Tokyo.
[||] National Defense Medical College.
[⊥] Tokyo University of Science.
[#] Department of Chemistry and Biotechnology, The University of Tokyo.
[+] CREST.
[@] Center for NanoBio Integration, The University of Tokyo.

(1) *Dendrimers and other Dendritic Polymers*; Fréchet, J. M. J., Tomalia, D. A., Eds.; John Wiley & Sons: New York, 2001.
(2) Bosman, A. W.; Janssen, H. M.; Meijer, E. W. *Chem. Rev.* **1999**, *99*, 1665−1688.
(3) Lee, I.; Athey, B. D.; Wetzel, A. W.; Meixner, W.; Baker, J. R., Jr. *Macromolecules* **2002**, *35*, 4510−4520.
(4) Roy, R.; Zanini, D.; Meunier, S. J.; Romanowska, A. *J. Chem. Soc., Chem. Commun.* **1993**, 1869−1872.
(5) Jang, W.-D.; Kataoka, K. *J. Drug Delivery Sci. Technol.* **2005**, *15*, 19−30.
(6) Wiener, E. C.; Brechbiel, M. W.; Brothers, H.; Magin, R. L.; Gansow, O. A.; Tomalia, D. A.; Lauterbur, P. C. *Magn. Reson. Med.* **1994**, *31*, 1−8.
(7) Malik, N.; Evagorou, E. G.; Duncan, R. *Anti-Cancer Drugs* **1999**, *10*, 767−776.
(8) Maruyama-Tabata, H.; Harada, Y.; Matsumura, T.; Satoh, E.; Cui, F.; Iwai, M.; Kita, M.; Hibi, S.; Imanishi, J.; Sawada, T.; Mazda, O. *Gene Ther.* **2000**, *7*, 53−60.

10.1021/cm071451m CCC: $37.00
Published on Web 10/11/2007

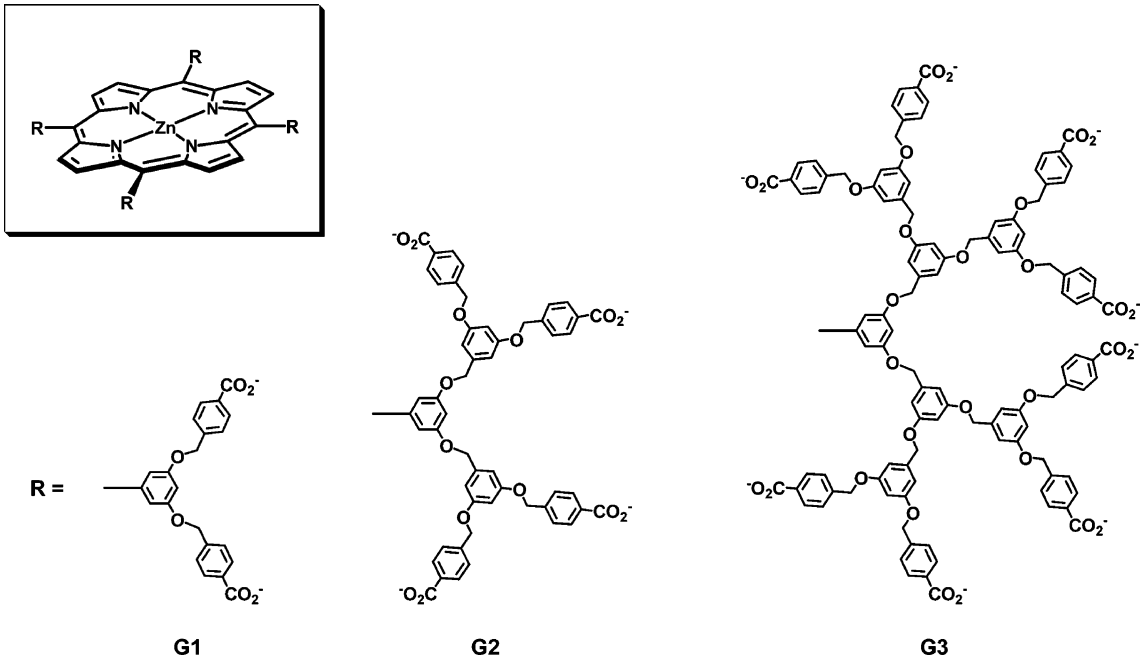

Figure 1. Structures of dendrimer porphyrins (DPs).

Table 1. Physical Properties of DP-Loaded PIC Nanocarriers

generation	hydrodynamic diameter (nm)[a]	polydispersity index (μ_2/Γ^2)	$M_{w,app}$ (10^5 g/mol)	association no. PEG-*b*-PLL/DP	CAC[b] (mg/mL)	ζ-potential (mV)
G1	126.5	0.131	2240	8989/32585	<0.1	1.11 ± 0.072
G2	78.0	0.249	100	399/722	<0.1	0.48 ± 0.31
G3	44.0	0.030	9.26	39/38	<0.1	-0.20 ± 0.57

[a] Cumulant diameter. [b] Critical association concentration.

activation by light at a wavelength matching the absorption wavelength of photosensitizer leads to the generation of reactive oxygen species (ROS) that causes the oxidative destruction of a target tissue.[12,13] As a revolutionary method in preclinical and clinical applications over the last few decades, numerous attempts have been made to improve the PDT efficacy. Among them, the creation of an efficient photosensitizer and its efficient delivery to the target tissue is an attractive topic. An ideal photosensitizer should have the following properties: (1) high quantum yield, (2) a large absorption cross-section, (3) good solubility in an aqueous medium, (4) no dark toxicity, and (5) preferential selectivity to the malignant tissue.[12−15] However, most of the photosensitizers developed in a preclinical or clinical study show poor water solubility with aggregate formation and skin phototoxicity due to a nonspecificity to tumors.[13,16]

On the basis of the above information, we have designed DPs as potential photosensitizers, because we expected that large dendritic wedges can effectively segregate the focal porphyrin cores and thereby prevent collisional quenching of the porphyrins even at a very high concentration.[9−11] In fact, the third generation DPs exhibited a remarkable PDT efficacy. In addition, ionic peripheral functionalities allow the formation of polyioncomplex (PIC) micelles with oppositely charged block copolymers.

In a present study, we investigated the systematic evaluation of the influence of the DP generation on the physicochemical properties and nanocarrier formation. A series of negatively charged DPs (Figure 1; Gn = n-generation dendrimer, $n = 1-3$)[11,17,18] with poly(ethylene glycol)-*block*-poly(L-lysine) (PEG-*b*-PLL)[19−21] were used to form the PIC nanocarriers.

Results

Formation of DP-Loaded PIC Nanocarriers. The DPs were synthesized by a previously reported method.[17] All of the dendrimers were unambiguously characterized by ^{1}H NMR and MALDI-TOF-MS measurements. The DPs clearly

(9) Nishiyama, N.; Stapert, H. R.; Zhang, G.-D.; Takasu, D.; Jiang, D.-L.; Nagano, T.; Aida, T.; Kataoka, K. *Bioconjugate Chem.* **2003**, *14*, 58−66.
(10) Zhang, G.-D.; Harada, A.; Nishiyama, N.; Jiang, D.-L.; Koyama, H.; Aida, T.; Kataoka, K. *J. Controlled Release* **2003**, *93*, 141−150.
(11) Jang, W.-D.; Nishiyama, N.; Zhang, G.-D.; Harada, A.; Jiang, D.-L.; Kawauchi, S.; Morimoto, Y.; Kikuchi, M.; Koyama, H.; Aida, T.; Kataoka, K. *Angew. Chem., Int. Ed.* **2005**, *44*, 419−423.
(12) Bonnettt, R. *Chemical Aspects of Photodynamic Therapy*; Gordon and Breach Science Publishers: Amsterdam, 2000.
(13) Pandey, R. K.; Zheng, G. In *The Porphyrin Handbook*; Kadishi, R. K., Smith, K. M., Guilard, R., Eds.; Academic Press: New York, 2000; Vol. 6, pp 157−230.
(14) Derycke Annelies, S. L.; Witte, P. A. M. *Adv. Drug Delivery Rev.* **2004**, *56*, 17−30.
(15) van Dongen, G. A. M. S.; Visser, G. W. M.; Vrouenraets, M. B. *Adv. Drug Delivery Rev.* **2004**, *56*, 31−52.
(16) Hamblin, M. R.; Newman, E. L. *J. Photochem. Photobiol., B* **1994**, *23*, 3−8.
(17) Sadamoto, R.; Tomioka, N.; Aida, T. *J. Am. Chem. Soc.* **1996**, *118*, 3978−3979.
(18) Aida, T.; Jiang, D.-L. In *The Porphyrin Handbook*; Kadishi, R. K., Smith, K. M., Guilard, R., Eds.; Academic Press: New York, 2000; Vol. 3, pp 369−384.
(19) Harada, A.; Kataoka, K. *Macromolecules* **1995**, *28*, 5294−5299.
(20) Harada, A.; Kataoka, K. *Science* **1999**, *283*, 65−67.
(21) Katayose, S.; Kataoka, K. *Bioconjugate Chem.* **1997**, *8*, 702−707.

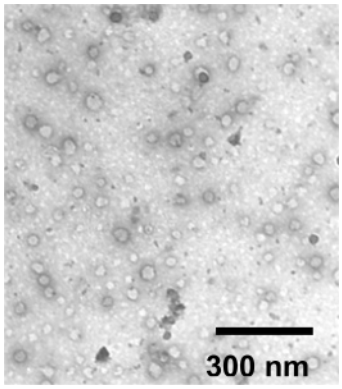

Figure 2. TEM images G3-loaded PIC nanocarriers.

formed multimolecular PIC assemblies (PIC nanocarriers) by mixing with PEG-*b*-PLL in aqueous solutions. As shown in Table 1, the DP-loaded PIC nanocarriers have almost neutral ζ-potential values, indicating a charge neutralization between the DPs and PEG-*b*-PLL to form PICs with a PEG palisade. The size and polydispersity index of the PIC nanocarriers, which were evaluated by DLS measurements, strongly depended on the generation number of the DPs (Table 1).[22] The G3-loaded PIC nanocarrier exhibits an average diameter of 44 nm and remarkably low polydispersity index ($\mu_2/\Gamma^2 = 0.030$), which is consistent with the core−shell-type micelle structure. The G2-loaded PIC nanocarrier had an average diameter of 78 nm and remarkably high polydispersity index ($\mu_2/\Gamma^2 = 0.249$), and the G1-loaded PIC nanocarrier showed a relatively large average diameter of 126 nm and a moderate polydispersity index ($\mu_2/\Gamma^2 = 0.131$). Also, the association numbers, apparent molecular weight ($M_{w,app}$), as well as the ζ-potential of the PIC nanocarriers are summarized in Table 1. The G3-loaded PIC nanocarrier was formed from 38 G3 and 39 PEG-*b*-PLL copolymers. The G2-loaded PIC nanocarrier had 1 order of magnitude higher association numbers and $M_{w,app}$ than those of the G3-loaded PIC nanocarrier. The G1-loaded PIC nanocarrier showed much higher association numbers and $M_{w,app}$ values than both the G-2 and the G-3 loaded species. The TEM image of the G3-loaded PIC nanocarriers showed spherical nanoparticles, indicating the formation of a core−shell-type micelle structure (Figure 2).

Time-Resolved Fluorescence Measurements. The aggregate formation of photosensitizers results in fluorescence quenching due to an increase in the nonradiative decay of the excited states.[23] Our previous studies[10,11] indicated that large dendritic wedges can successfully prevent the quenching of photosensitizers by steric isolation. In this context, time-resolved fluorescence decay curves of the DPs and DP-loaded PIC nanocarriers were recorded to obtain information about the effect of collisional quenching of the focal porphyrin units within the self-assembled PIC systems. As shown in Figure 3, the free DPs exhibit almost comparable fluorescent decay profiles, indicating that DPs have high solubility in aqueous medium and mostly exist in monomeric

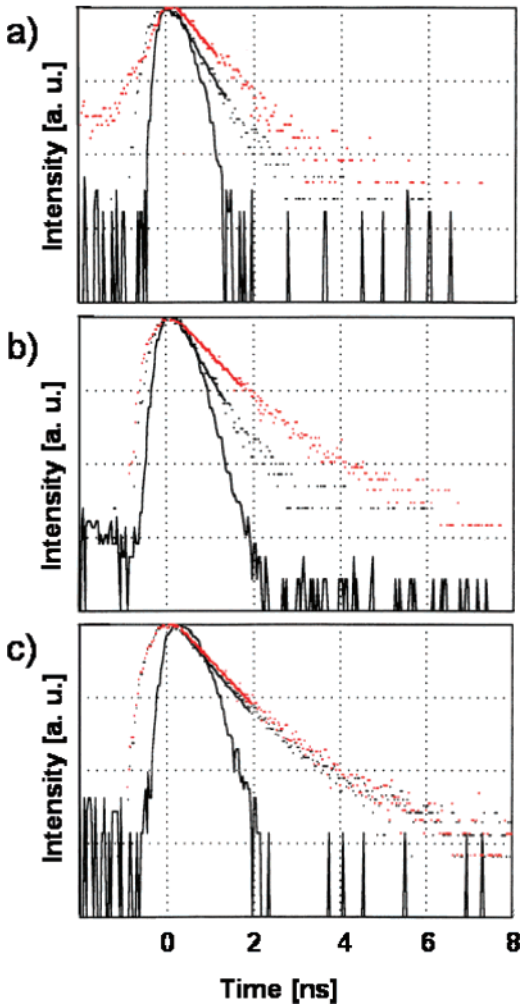

Figure 3. Fluorescence decay curves of G1 (a), G2 (b), and G3 (c) DPs (red line) and DP-loaded PIC nanocarriers (black line).

state. Within the PIC nanocarriers, the G1- and G2-loaded PIC nanocarriers exhibit a significant fluorescence quenching signature as compared to the corresponding free DPs. In sharp contrast, the G3-loaded PIC nanocarrier showed almost comparable decay rates to the free G3 (Figure 3c). This result supports our assumption that the large dendritic wedges can prevent the collisional quenching of the photosensitizing units, whereas the relatively small dendritic architecture cannot perfectly prevent the collisional quenching of the focal porphyrin units within the core of PIC nanocarriers.

Oxygen Consumption Abilities. The photoinduced oxygen consumption of the DPs and DP-loaded PIC nanocarriers was observed to evaluate the efficiency of the photochemical reactions. Under light irradiation, photosensitizers produce ROS involving singlet oxygen and the superoxide anion. The partial oxygen pressure (PO_2) change in the medium containing DPs or PIC nanocarriers with 10% FBS was recorded during photoirradiation. As shown in Figure 4, the G3 and G3-loaded PIC nanocarrier exhibit similar oxygen consumption amounts. In contrast, the oxygen consumption amount appreciably decreased when the G2 or G1 DP was loaded into the nanocarriers. Without 10% FBS, both the DPs and the DP-loaded PIC nanocarriers showed an almost negligible change in the PO_2 upon photoirradiation (data not shown),

(22) Burchard, W. In *Light Scattering: Principles and Development*; Brown, W., Ed.; Clarendon Press: New York, 1996.
(23) Lakowicz, J. R. *Principles of Fluorescence Spectroscopy*; Kluwer Academic/Plenum Publishers: New York, 1999.

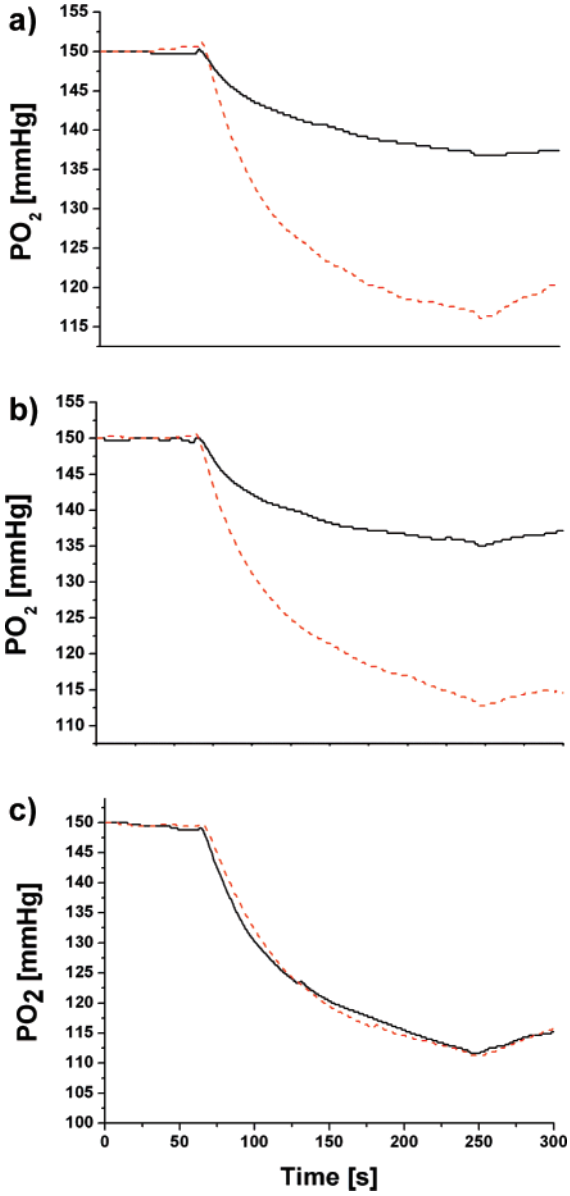

Figure 4. Oxygen partial pressure change of medium included G1 (a), G2 (b), and G3 (c) DPs (− − −) and DP-loaded PIC nanocarriers (−).

indicating that the proteins in FBS act as sacrificial acceptors of ROS.

Cellular Uptake. Efficient cellular association of a photosensitizer could lead to a high PDT efficacy. To quantitatively evaluate the cellular uptake of DPs and DP-loaded PIC nanocarriers, HeLa cells were incubated with 6.25 μM DPs or DP-loaded PIC nanocarriers having an equivalent amount of DPs (Figure 5). The cellular uptake of DPs is significantly enhanced by the incorporation into nanocarriers, indicating that the anionic surface of the DPs results in a limited interaction with a negatively charged cellular membrane. Charge neutralization and shielding of the PICs by the PEG segment might reduce the electrostatic repulsion with a cell. Therefore, encapsulation of the DPs into the PIC nanocarriers might be effective for the intracellular delivery of DPs.

The uptake amount of DPs showed a strong generation dependence. Interestingly, the G1-loaded PIC nanocarrier shows the largest uptake amount, while the G3-loaded PIC

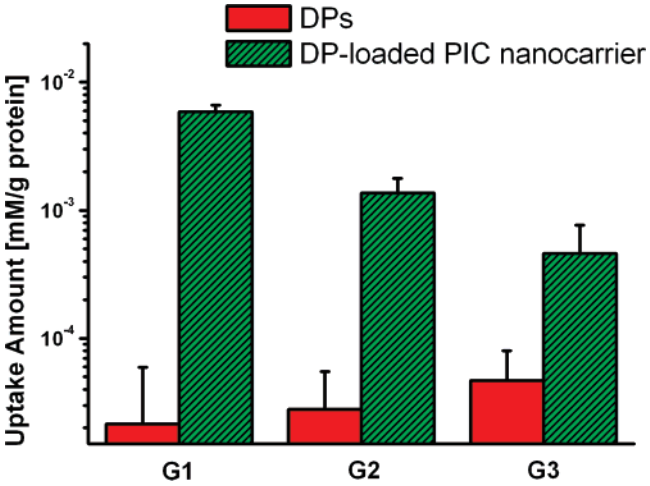

Figure 5. Cellular uptake amount of DPs and DP-loaded PIC nanocarriers. 6 μM DPs or DP-loaded PIC nanocarriers with equivalent amount of DPs is incubated.

nanocarrier gave the lowest uptake amount among the three DP-loaded PIC nanocarriers. The difference in the cellular uptake between generations is possibly caused from the morphological difference in the nanocarriers, such as the size, association number, and stability of the PICs.

Photodynamic Effect. The in vitro photodynamic effect against HeLa cells was evaluated by the MTT assay. The DPs and the DP-loaded PIC nanocarriers showed an almost negligible cytotoxicity under dark conditions (data not shown), whereas each species exhibited a strong photocytotoxicity. Figure 6 shows the cell viability−concentration curve, where the DPs apparently exhibit a remarkable increase in the photocytotoxicity by incorporation into the nanocarriers. Fifty percent inhibitory concentrations (IC_{50}) of the DPs and DP-loaded PIC nanocarriers, the concentration of photosensitizer at which 50% mortality of tumor cells as compared to the control was observed after a photoirradiation, were calculated from the cell viability−concentration curve (Table 2). The G1- and G2-loaded PIC nanocarriers exhibited 7.5 and 50 times, respectively, higher photocytotoxicities as compared to the G1 and G2 DPs. Notably, the G3-loaded PIC showed a 167 times enhanced photocytotoxicity as compared to free G3 DP.

Discussion

All of the DPs showed high solubility in aqueous medium due to the ionic charges of dendritic wedges. When the DPs are mixed with PEG-*b*-PLL copolymers in a stoichiometric ratio, positively charged PLL segments successfully interact with negative surface functionalities of DPs to form the DP-loaded PIC nanocarriers. The values of the ζ-potential also well coincide with the charge neutralization between the DPs and PEG-*b*-PLL as well as encapsulation of the PICs within the PEG layer.

Notably, the PIC nanocarriers had a high stability upon dilution with a very low critical association concentration being observed. These features are significantly important parameters from a therapeutic point of view. For target delivery of the therapeutic agent, the drug formulation should have a tolerance against dilution and maintain long circula-

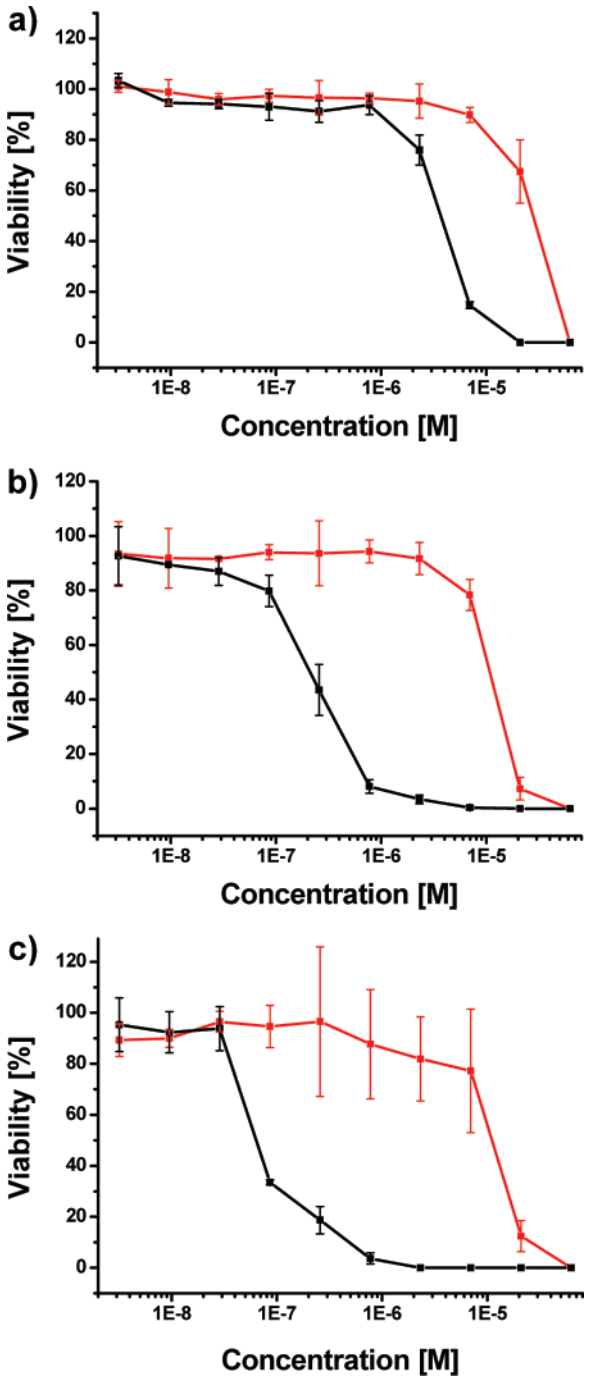

Figure 6. The viability of Hela cells treated with G1 (a), G2 (b), and G3 (c) DPs (red line) and DP-loaded PIC nanocarriers (black line).

Table 2. IC_{50} of DPs and DP-Loaded PIC Nanocarriers (unit: M)

generation	DP	DP-loaded PIC nanocarrier
G1	3.0×10^{-05}	4.0×10^{-06}
G2	1.2×10^{-05}	2.0×10^{-07}
G3	1.0×10^{-05}	6.0×10^{-08}

tion times in the blood stream. Also, the PIC nanocarriers may facilitate targeting to tumor tissues by the so-called enhanced permeability and retention (EPR) effect.[24]

The DLS measurement of the DP-loaded PIC nanocarriers exhibited a generation dependence, where the G3-loaded PIC nanocarrier showed a nicely dispersed particle formation with a diameter of 44 nm. The sizes of the G1- and G2-loaded PIC nanocarriers are generally larger than that of the G3-loaded PIC nanocarrier. TEM observations of the G3-loaded PIC nanocarrier showed a spherical assembly formation, which is consistent with the core−shell-type micelle structure. In contrast, the G2- or G1-loaded PIC nanocarrier showed a high polydispersity. The difference in size and distribution might be attributable to the number of anionic charges and dendritic architecture. The relatively open architecture of the G1 and G2 cannot perfectly prevent $\pi-\pi$ interactions among the porphyrin cores when they form the PICs. Thus, the association of the DPs with a low generation is possibly driven by the $\pi-\pi$ interaction as well as an electrostatic interaction.

In the photodynamic process sequence, the DPs are converted to excited state under light irradiation, and then they transfer excited energy or electrons to oxygen molecules to generate the ROS. The time-resolved fluorescence observation provides information about the energy transduction procedure, and the oxygen consumption ability is directly related to the ROS generation. The fluorescence decay and oxygen consumption profiles of each DP did not have large differences among the differnet generation of DPs (Figures 3 and 4). Also, the cellular uptake and photocytotoxicity of DPs were almost comparable values regardless of the generation of DPs (Figures 5 and 6). A molecular aggregation of the photosensitizers might result in the fluorescence quenching behavior. All of the free DPs exhibit almost comparable fluorescence decay profiles, indicating that DPs are succesfully segregated within aqueous medium due to high solubility and charge repulsion of surface carboxylic acid functionalities. On the other hand, the G1 and G2 showed a significant fluorescence quenching by incorporation into the PIC nanocarriers (Figure 3), indicating that the G1 and G2 have high proportions of nonradiative decays within the PIC nanocarriers by collisional quenching. Also, the G1- or G2-loaded PIC nanocarriers exhibited a significant decrease in their oxygen consumption ability as compared to the free DPs (Figure 4). We noted that either the DPs or the DP-loaded PIC nanocarrier solution without 10% FBS showed almost negligible changes in the PO_2 upon photoirradiation, indicating that the proteins in FBS act as sacrificial acceptors of the ROS. In other words, if proteins do not exist in the medium, once generated, the ROS promptly revert to the ground-state oxygen molecules due to their short lifetimes. This fact means that the reduced oxygen consumption of the G1- or G2-loaded PIC nanocarrier is possibly caused by the increase in the nonradiative decays of the excited states and also the generation of less reactive ROS. Additionally, the diffusivity of oxygen molecules is possibly reduced within the G1- and G2-loaded PIC nanocarriers due to their large hydrodynamic size. In contrast, the G3-loaded PIC nanocarrier showed an almost comparable fluorescence decay profile (Figure 3) and oxygen consumption to the free G3 (Figure 4), indicating that the third generation dendritic wedges can sufficiently prevent aggregation of the photosensitizing porphyrin units, and the G3 can efficiently transfer excited energy to oxygen molecules without loss even in a highly concentrated state of G3 in the PIC nanocarrier. Also,

(24) Maeda, H.; Wu, J.; Sawa, T.; Matsumura, Y.; Hori, K. *J. Controlled Release* **2000**, *65*, 271−284.

Table 3. The Change of Parameters of DPs by Inclusion into the PIC Nanocarriers in Each Generation System

generation	fluorescence lifetime	oxygen consumption	uptake ratio (*A*)	photocytotoxicity ratio (*B*)	*B*/*A*
G1	shortened	decreased	95	7.5	0.079
G2	shortened	decreased	53	50	0.94
G3	maintained	no change	15	167	11.1

the ROS generated from the G3-loaded PIC nanocarrier can efficiently react with serum proteins in the media.

Positively charged particles might have a large affinity against cell membranes, but the cationic particles easily associate with the negatively charged serum proteins such as albumin. Therefore, DPs with an anionic periphery may have a high availability from a clinical point of view as compared to the positively charged ones. Furthermore, the formation of the PIC nanocarriers may prevent aggregate formation during the blood circulation due to the steric stabilization of the PEG shell layer. Also, the formation of the PIC nanocarriers may improve the uptake amount of the DPs by the charge neutralization. In fact, DP-loaded PIC nanocarriers showed an appreciably high level of uptake as compared to the free DPs (Figure 5). Correspondingly, the photocytotoxicity of each PIC nanocarrier was remarkably improved as compared to that of the free DPs (Figure 6). One of the interesting aspects in this regard is the enhanced photocytotoxicity of the PIC nanocarriers encapsulating DP with an increased generation despite the generation-dependent relative decrease in their uptake amount of PIC nanocarriers.

To evaluate the effect of the DP generations on the PDT efficacy, various parameter changes after the incorporation of the DPs into the PIC nanocarriers are summarized in Table 3. The cellular uptake and photocytotoxicity ratios are obtained by normalization of the cellular uptake amount and the IC_{50} of the DP-loaded PIC nanocarriers by those of the free DPs. Additionally, the photocytotoxicity ratio is normalized by the uptake ratio for calculating the PDT efficacy of the individual DPs (*B*/*A*). G1 shows the reduced PDT efficacy by incorporation into the PIC nanocarriers. This is consistent with the shortened lifetime and decreased oxygen consumption of the G1-loaded PIC nanocarrier. However, the G2-loaded PIC nanocarrier exhibits a comparable PDT efficacy with the free G2 despite the shortened fluorescent lifetime and decreased oxygen consumption. Notably, the incorporation of the G3 into the PIC nanocarrier shows an 11-fold enhancement of the PDT efficacy. The high local concentration of DPs within the core of PIC nanocarrier is able to generate a large amount of ROS at a local site, which may lead to a high photochemical oxidation level and easily overcome the photodynamic threshold. Also, there is a possibility to change the subcellular localization of DPs by the formation of PIC nanocarriers. It should be noted in this regard that the pegylated chlorin-e6 as well as the PEG-based polymeric micelles were recently reported to show an enhanced localization in several cytoplasmic organelles including the mitochondria.[25,26] Now, we are going to observe the subcellular localization of the DPs to investigate detailed mechanism of the enhanced PDT efficacy.

Consequently, in the present investigation, we were able to determine that the PDT efficacy is highly dependent on the generation of the DPs when they formed PIC nanocarriers. The PIC nanocarriers formed from large DPs produced a high quantum yield of ROS generation and a strong nanocarrier effect, resulting in a high PDT efficacy.[27]

Conclusions

This study was conducted to systematically investigate the effect of the dendritic structures of DPs on the physicochemical property, cellular uptake, and PDT efficacy. A dendrimer generation-dependent PDT efficacy was revealed by the inclusion of DPs into supramolecular nanocarriers of PICs. To summarize the results in the present Article, we can consider the following several parameters to design effective photosensitizers: (1) Large dendritic wedges form uniform core−shell PIC micelles. (2) PIC nanocarrier formation enhances cellular uptake. (3) Incorporation of DPs in nanocarrier systems may provide enhancement of the photodynamic efficacy. In this way, G3 with a large dendritic structure encapsulated into the PIC micelles would be an ideal photosensitizer and may have a high utility for in vivo PDT applications.

Acknowledgment. This study was supported by the Industrial Technology Research Grant Program in ’04 from the New Energy and Industrial Technology Development Organization (NEDO) of Japan. Y.L. acknowledges the JSPS Young Scientist Fellowship.

Supporting Information Available: Materials and detailed experimental procedures (PDF). This material is available free of charge via the Internet at http://pubs.acs.org.

CM071451M

(25) Hamblin, M. R.; Miller, J. L.; Rizvi, I.; Ortel, B.; Maytin, E. V.; Hasan, T. *Cancer Res.* **2001**, *61*, 7155−7162.
(26) Savic, R.; Luo, L.; Eisenberg, A.; Maysinger, D. *Science* **2003**, *300*, 615−618.
(27) Ideta, R.; Tasaka, F.; Jang, W.-D.; Nishiyama, N.; Zhang, G.-D.; Harada, A.; Yanagi, Y.; Tamaki, Y.; Aida, T.; Kataoka, K. *Nano Lett.* **2005**, *5*, 2426−2431.